J Appl Electrochem (2008) 38:1135–1142
DOI 10.1007/s10800-008-9549-8

ORIGINAL PAPER

NO reduction performance of Rh paste catalyst on YSZ under steady state and forced oscillation electropromotion conditions

S. Brosda · C. G. Vayenas

Received: 29 October 2007 / Revised: 5 March 2008 / Accepted: 7 March 2008 / Published online: 26 March 2008

Abstract The technique of cyclic voltammetry was applied in conjunction with on-line catalytic product analysis to investigate the electrochemical promotion of NO reduction by C_3H_6 in presence of O_2 on Rh catalyst-electrode films on YSZ at temperatures 350–490 °C. Cyclic linear potential sweep amperometry under catalytic reaction conditions leads to cyclic non-Faradaic electrochemical modifications in the CO_2 formation and NO reduction rates which are compared to those obtained under steady state potentiostatic operation.

Keywords NO reduction · Rh catalyst electrode · Cyclic voltammetry · AC impedance spectroscopy

1 Introduction

The high catalytic activity of Rh catalyst-electrodes for NO reduction is well known and its electrochemical promotion [1–3] has been studied intensively with respect to (a) its oxygen and hydrocarbon partial pressure dependence [4, 5], (b) the role of surface Rh_2O_3 formation [6–8] and (c) its practical utilization [5, 9, 10].

The CO_2 and N_2 formation rates are enhanced both with positive (anodic) and negative (cathodic) potentials and currents [4, 5, 11, 12]. This type of rate dependence on potential is known as inverted volcano type behaviour [5]. The observed very pronounced promotional phenomena can be understood by taking into account the effect of potential and concomitant changes in work function [12, 13] on the chemisorptive bond strength of all three co-adsorbates, i.e. oxygen, propylene and NO. At high anodic potentials, in particular, the Rh=O bond is weakened and enables NO to adsorb and dissociate even in presence of co-adsorbed oxygen. At high cathodic potentials, the chemisorptive bond of propylene is weakened and therefore NO adsorption and dissociation is enhanced [5].

The technique of cyclic voltammetry (CV) is used routinely in aqueous electrochemistry to study the mechanism of electrocatalytic reactions. In solid state electrochemistry, CV is mainly used for corrosion studies and for studying O_2 adsorption/reduction phenomena on noble metal electrodes [14–17]. There have been two earlier publications, where catalytic reactions were investigated under such forced oscillation conditions [17, 18]. Vayenas et al. [17], for example, studied the ethylene oxidation on Pt/YSZ while a linear potential sweep was imposed to the catalyst-electrode. During this potential sweep with a small scan rate of only 5 mV s^{-1}, the rate of CO_2 formation increases in the anodic branch of the cycle and shows clearly a non-Faradaic increase in the rate (electrophobic type of reaction). In that study [17] the vertex potentials of ± 0.5 V were rather small in comparison to potentiostatic transient experiments (up to ± 2 V) and the hysteresis in the CO_2 production rate in the forward and backward scan was small. A pronounced oxygen reduction cathodic peak in the $I–U_{WR}$ plot of the CV was observed and became even more pronounced at significant higher scan rates (40–90 mV s^{-1}). It corresponds to oxygen adsorbed on the catalyst under reaction conditions.

In this study the solid electrolyte cyclic voltammetry (SECV) technique is applied to a porous Rh catalyst-electrode exposed to a reactive gas mixture of NO, propylene and oxygen and serving as a catalyst for NO reduction and propylene oxidation. The purpose of this investigation was to (1) examine whether SECV can provide in situ information

S. Brosda · C. G. Vayenas (✉)
Department of Chemical Engineering, University of Patras, Caratheodry St. 1, 26500 Patras, Greece
e-mail: cat@chemeng.upatras.gr

about chemisorbed species and the redox-couple $Rh^0 \leftrightarrow Rh^{3+}$, (2) to examine if SECV can be used as a fast initial test of the NO reduction performance of Rh catalysts and (3) to examine if time-averaged electropromotion performance under cyclic operation can exceed the performance under steady state polarization.

2 Experimental

The experimental setup consists of the flow system, the reactor and the gas analysis units. The reactor corresponds to the "single chamber" design [5, 12].

The Rh metal film deposited onto one side of the YSZ pellet serves as the working electrode while two Au films deposited on the other side of the pellet serve as the reference and counter electrode. All three electrodes are exposed to the same gas mixture. The Rh catalyst film was deposited on one side of the YSZ pellet by application of a thin coating of Engelhard Rh paste A-8826, followed by calcination in air at 550 °C and an in situ reduction during heating from 150 to 450 °C in a mixture of 2.5% H_2 in He (150 mL min^{-1}) while monitoring the in-plane Rh film resistance, i.e. the resistance between two points at opposite ends of the 1 cm × 1 cm film. The metal film obtained exhibits adequate conductivity for NEMCA experiments, since its in-plane resistance is low enough, i.e. in the range of 5–20 Ω [5]. The true surface area of the 1 cm × 1 cm film, (expressed in surface mol Rh, N_{Rh}), estimated from catalytic rate transient time constant, τ, during galvanostatic transients (C_2H_4 oxidation) via the expression $\tau = 2FN_{Rh}/I$, was found to be 1.4×10^{-6} mol Rh. This value indicates a roughness factor of the order of 700 which is comparable with those (50–500) of Pt paste films used in electrochemical promotion studies [1, 2, 12].

Reactants were L′ Air Liquide certified standards of C_3H_6 and O_2 in He which were further diluted with ultrapure He (99.999%) also supplied by L′ Air Liquide. The reaction mixture was fed to the continuous flow atmospheric pressure reactor with a volume of 30 cm^3 and has been shown to exhibit CSTR behaviour over the flow range of 50–250 cm^3 STP min^{-1} [1, 2, 12].

The on-line analysis unit consisted of a GC (Shimadzu 14-A) fitted with a TCD and Porapak QS column (NO, N_2O, CO_2, C_3H_6) and moleculare sieve (N_2, O_2), a Rosemont IR CO_2 analyzer, and a Teledyne 911/912 NO/NO_x analyzer. The voltage output signal from the CO_2 and NO analyzer was recorded using a Yokogawa LR4220 pen recorder. No measurable rates of N_2O or CO formation were observed under steady state or forced oscillation conditions over the investigated temperature and feed gas composition range. Thus the rates of CO_2 and N_2 formation, r_{CO_2} and r_{N_2}, respectively, expressed in mol O s^{-1} were computed from the appropriate mass balances:

$$r_{CO_2} = G y_{CO_2} \quad (1)$$

$$r_{N_2} = (1/2) G (y_{NO,\,feed} - y_{NO}) \quad (2)$$

where G (mol s^{-1}) is the total molar flow rate through the reactor, which is practically constant due to the high reactant dilution. As already noted the residence time distribution of the reactor is very close to that of a CSTR [1, 2, 12].

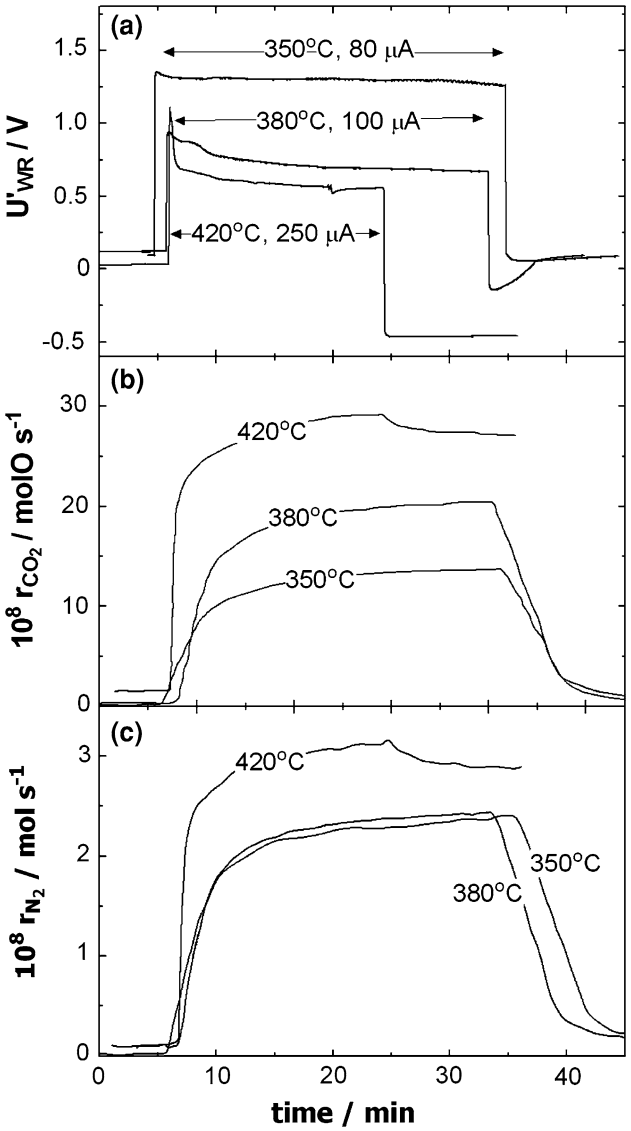

Fig. 1 Galvanostatic transients at 350, 380 and 420 °C (**a**) potential during current application of applied current, I, 80, 100 and 250 μA, respectively, (**b**) CO_2 formation (**c**) N_2 formation rate during transient operation. Conditions: $p_{NO} = p_{C_3H_6} = 0.1$ kPa, $p_{O_2} = 0.2$ kPa flow rate, F = 185 cm^3 STP min^{-1}

Table 1 Steady state open circuit rates, $r^{o}_{CO_2}$ and $r^{o}_{N_2}$, rate enhancement ratios, $\rho^{o}_{CO_2}$ and ρ_{N_2}, and Faradaic efficiencies, Λ_{CO_2} and Λ_{N_2}, for the galvanostatic transients presented in Fig. 1

	350 °C	380 °C	420 °C
$r^{o}_{CO_2}$ (mol s^{-1})	3.5×10^{-10}	3.1×10^{-9}	1.5×10^{-8}
$r^{o}_{N_2}$ (mol s^{-1})	1.8×10^{-10}	1.0×10^{-9}	1.1×10^{-9}
$\rho^{o}_{CO_2}$	390	66	19
ρ_{N_2}	134	24	29
Λ_{CO_2}	165	194	106
Λ_{N_2}	58	45	24

The space time of the reactor (volume 30 cm^3) was 10 s and the mean residence time was typically 4 s. The fastest cycle during forced oscillations has a duration of 75 s, thus Eqs. 1 and 2 can be safely used to compute the instantaneous rates from G and the continuously recorded y_{CO_2} and y_{NO} values.

Currents or potentials were applied by means of a Solartron electrochemical interface 1286. AC impedance spectra were recorded under open circuit and polarization conditions using a Solartron SI 1255 frequency response analyzer and a 1286 electrochemical interface. Spectra were recorded at reaction steady-state in the frequency range 10^5–0.01 Hz with an a.c. amplitude of 20 mV.

3 Results and discussion

3.1 Electropromotion with fixed applied current or potential

Figure 1 shows a set of three typical galvanostatic NEMCA experiments demonstrating the transient effect of constant positive current application on the rates of CO_2 formation r_{CO_2} and NO reduction, r_{N_2}, and on the catalyst potential U_{WR} at 350, 380 and 420 °C. For all three temperatures the electrochemically induced increase in the rates of NO reduction to N_2 and propylene oxidation to CO_2, r_{N_2} and r_{CO_2}, respectively, is pronounced and strongly non-Faradaic and that the rate enhancement ratios, ρ_{N_2}, ρ_{CO_2} and Faradaic efficiencies, $\Lambda_{N_2}, \Lambda_{CO_2}$, decrease with increasing temperature (Table 1). Such galvanostatic transients are discussed in detail in [2]. For the present study it is more interesting to examine the corresponding catalyst potential with respect to the reference electrode response, U'_{WR}, for the case of 420 °C in Fig. 1 (We use U_{WR} for the IR-corrected potential and U'_{WR} for the non IR-corrected U_{WR} value). When the current of 250 μA was first applied to the sample, the catalyst potential increased from 0.05 to 1.1 V then fell rather abruptly to 0.6 V, indicating a change in the oxidation state at the Rh electrode surface. This behaviour is quite common when the catalyst surface is initially oxidized. The open circuit potential was 0.05 V before current application but dropped to −0.45 V immediately after

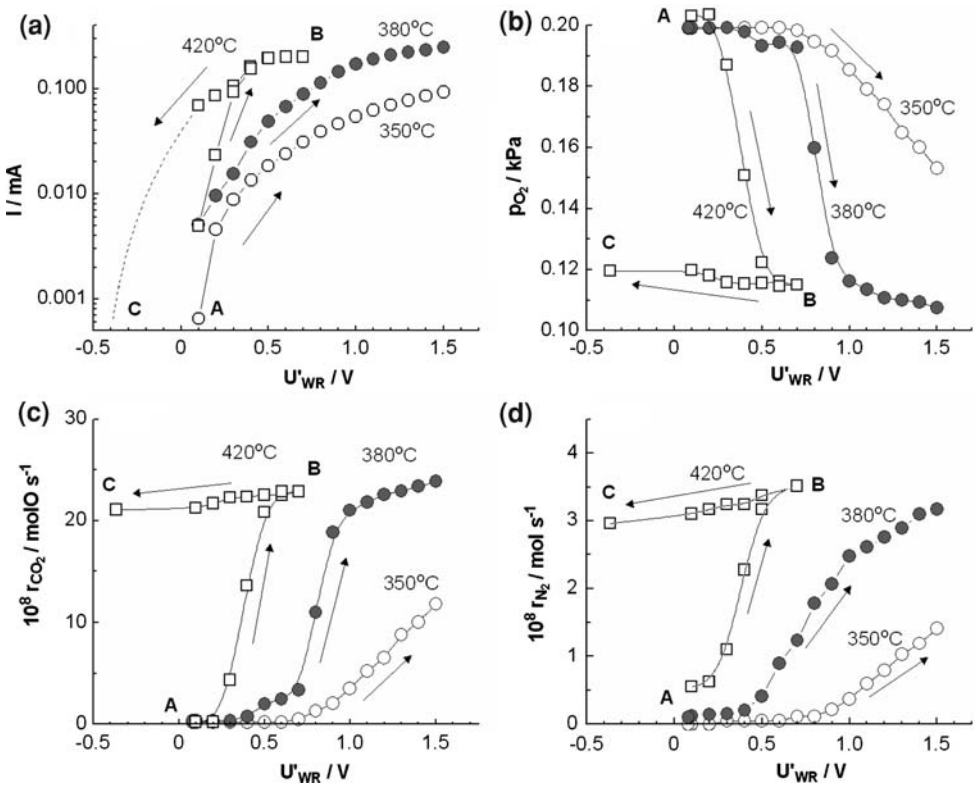

Fig. 2 Tafel plots (**a**), corresponding oxygen outlet partial pressure (**b**), corresponding catalytic CO_2 (**c**) and N_2 (**d**) formation rate dependence on catalyst potential U'_{WR}. See text for discussion. Conditions as in Fig. 1

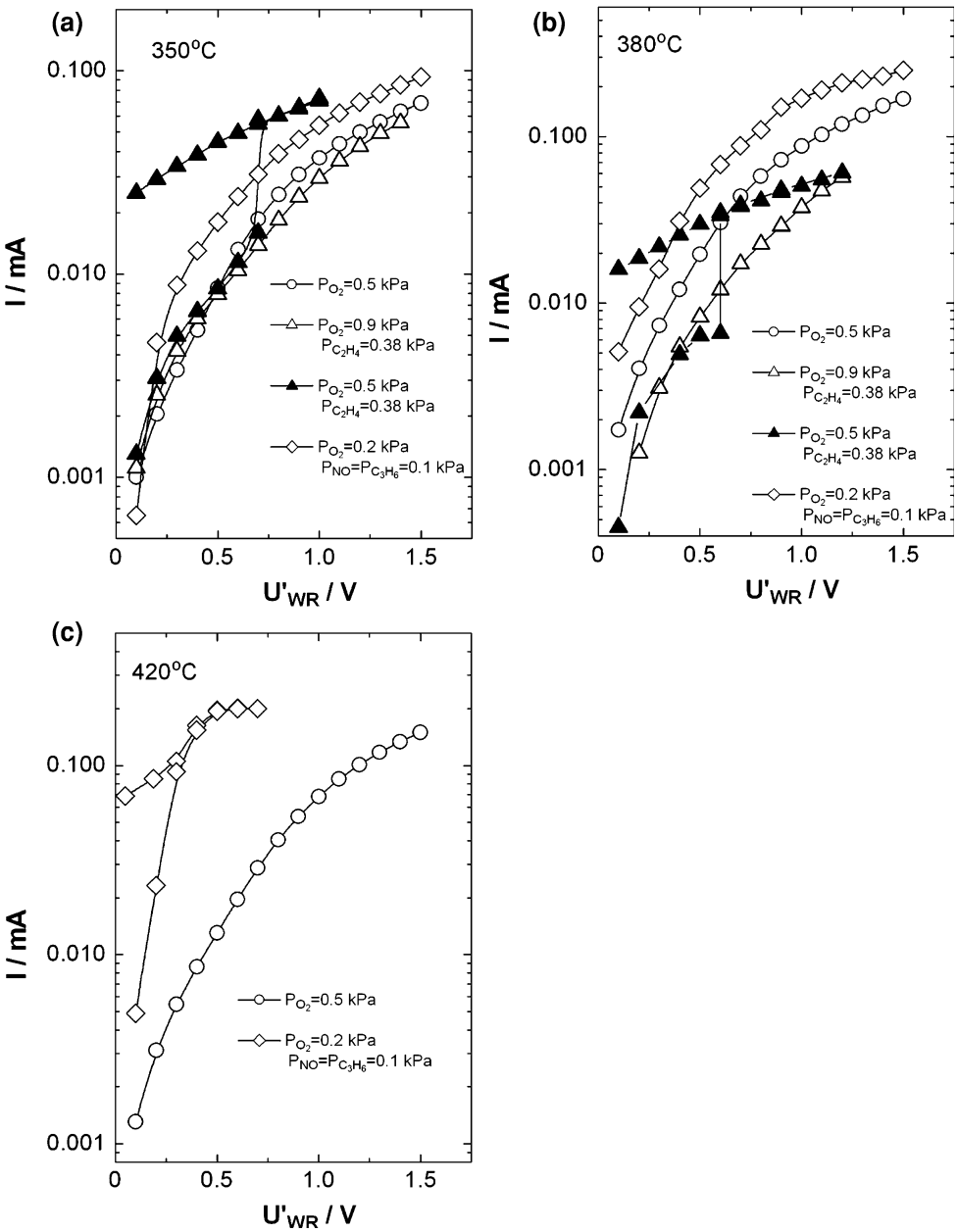

Fig. 3 Tafel plots at 350 °C (**a**), (380 °C (**b**) and 420 °C (**c**) under different reaction conditions: (○) $p_{O_2} = 0.5$ kPa, (Δ)$p_{O_2} = 0.9$ kPa, $p_{C_2H_4} = 0.38$ kPa, (▲) $p_{O_2} = 0.5$ kPa, $p_{C_2H_4} = 0.38$ kPa (◇) $p_{O_2} = 0.2$ kPa, $p_{NO} = p_{C_3H_6} = 0.1$ kPa

current interruption, indicating that the catalyst surface was indeed reduced to metallic Rh. Figure 1b and c show that under this new open circuit potential value at 420 °C, the rates of CO_2 and N_2 formation did not return to their initial values but remained very high. This pronounced hysteresis (very similar to permanent NEMCA [6, 15]) is also shown in Fig. 2, which presents results of steady state measurements carried out potentiostatically with anodic polarization at 350, 380 and 420 °C.

3.2 I–U curves with fixed applied current or potential

In Fig. 2a Tafel plots demonstrate at 350 and 380 °C the common exponential increase in current with applied potential, U'_{WR}, while at 420 °C and a potential of $U'_{WR} = 0.4$ V (point A–B) an abrupt increase in current and resulting rate of CO_2 formation (Fig. 2c) is observed. The open circuit potential after anodic polarization has changed dramatically to $U'_{WR} = -0.45$ V (point C) versus 0.05 V (point A) before potential application and a "permanent" NEMCA behaviour is observed, as in the galvanostatic transient in Fig. 1 for 420 °C. In Fig. 2a–d results are presented as function of the applied potential, U'_{WR}, which has been imposed between the working (Rh catalyst) and the reference electrode and the resulting Tafel plot for 420 °C also exhibits hysteresis. In principle for each point in the Tafel plot the concomitant overpotential, η, can be calculated from

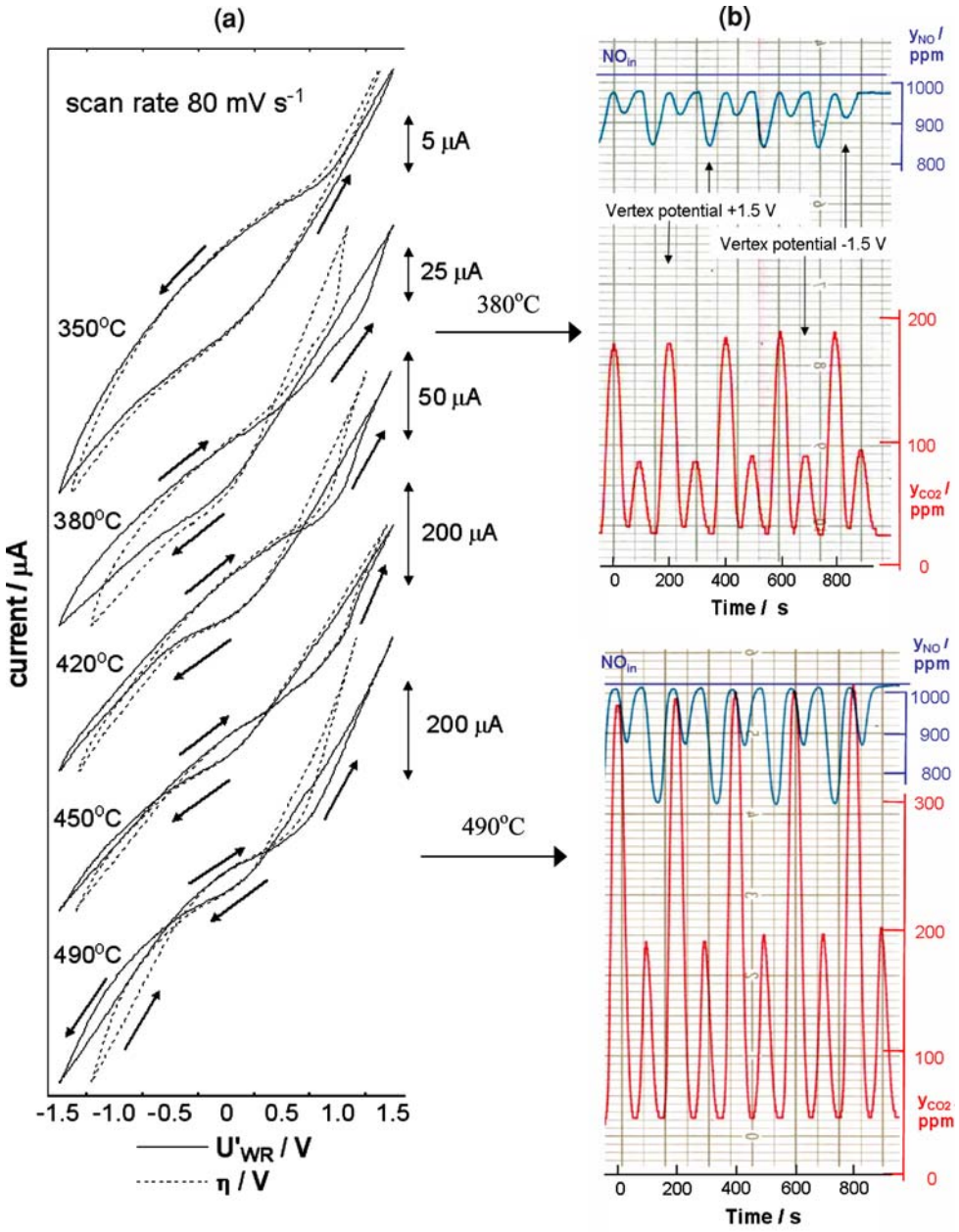

Fig. 4 (**a**) Solid electrolyte voltammetry (SECV) under catalytic reaction conditions: Series of cyclic voltammograms at different temperatures, scan rate 80 mV s^{-1}, (**b**) time variation of the CO_2 and NO concentration changes in five consecutive cycles, cyclic voltammograms obtained with a scan rate of 30 mV s^{-1}, vertex potential ±1.5 V, Conditions for (**a**) and (**b**) as in Fig. 1

$$\eta = U'_{WR} - U^{o}_{WR} - IR \tag{3}$$

taking into account the pronounced changes in the open circuit potential, U^{o}_{WR} and the total Ohmic resistance of the electrochemical cell via the IR-drop technique. However, the hysteresis and multiplicities in current and rates for the case of T = 420 °C are more easily observed and understood by plotting the results as a function of applied potential, U'_{WR} rather than η.

Figure 2b presents the oxygen outlet partial pressure, $p^{out}_{O_2}$, calculated from the mass balance of the two following stoichiometric reactions:

$$C_3H_6 + 4.5\,O_2 \rightarrow 3\,CO_2 + 3\,H_2O \tag{4}$$

$$2\,NO \rightarrow N_2 + O_2 \tag{5}$$

since no measurable N_2O formation was observed.

Figure 2b shows, that for 380 and 420 °C, $p^{out}_{O_2}$ decreases rapidly upon increasing the potential to 0.8 and 0.4 V, respectively, i.e. when the surface Rh_2O_3 is reduced [12]. The oxidation/reduction reaction $Rh^0 \leftrightarrow Rh^{3+}$ is reversible and the two catalytic states of the Rh catalyst (point A, oxidized and point C, reduced) can be obtained at will by changes in temperature, oxygen partial pressure and anodic/cathodic polarization.

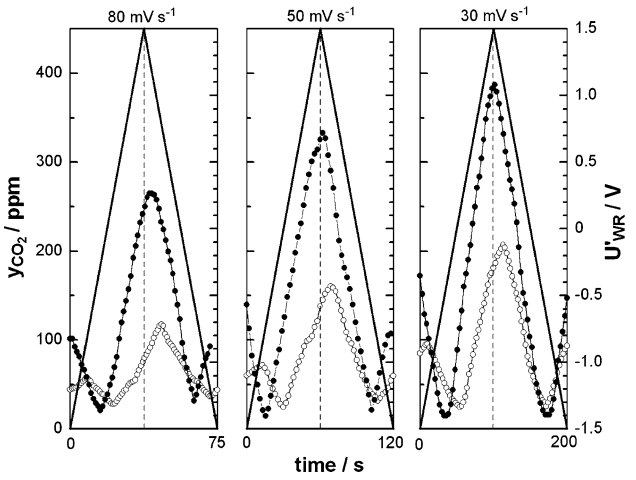

Fig. 5 Time variation of imposed catalyst potential, U'_{WR}, and resulting catalytic changes in CO_2 concentration. (○) T = 380 °C and (●) T = 490 °C. The last of five consecutive cycles is always shown. Conditions as in Fig. 1

In summary, Fig. 2 demonstrates the stability limit of the redox couple $Rh^0 \leftrightarrow Rh^{3+}$ as a function of temperature, $p_{O_2}^{out}$ and applied anodic potential at given reaction conditions of $p_{NO} = p_{C_3H_6} = 0.1$ kPa, $p_{O_2} = 0.2$ kPa and constant flow rate.

Figure 3 shows the effect of gaseous composition on the Tafel-plots. As expected, low p_{O_2} values stabilize the high current (reduced) state of the Rh catalyst while high p_{O_2} values favour the low current (oxidized) state. Cyclic voltammetric studies were therefore carried out mainly at 380 °C and with fast scan rates to avoid "permanent" NEMCA behaviour in which case the rates cannot be further changed by imposing a potential sweep.

3.3 Cyclic operation

CV potential sweeps under reaction conditions were run at temperatures between 350 and 490 °C using an imposed voltage from +1.5 to −1.5 V and scan rates of 30, 50 and 80 mV s^{-1}. The CO_2 formation and NO reduction performance was recorded at the same time in five consecutive cycles. Figure 4a shows a series of such CVs. Arrows indicate the forward and backward scan. In all cyclic voltammograms no distinct anodic or cathodic peak occurs but the anodic and cathodic potential scans are quite different. At 380 and 420 °C, the forward and backward scans intersect in the anodic region and at higher temperatures the forward and backward scans intersect even twice, at anodic and cathodic potentials. The crossover of the forward and backward curves in the cyclic voltammograms are associated in electrochemistry [19] with changes in the redox state of the catalyst electrode, which in the present study is the redox couple Rh^0 and Rh^{3+}.

AC impedance spectra were taken in the temperature range of 350–490 °C. Two distinct semicircles have been observed at all temperatures. The intersection of the first semicircle in the high frequency range with the *X*-axis has been used for the calculation of the total Ohmic resistance of the cell. These resistance values have been further used for the IR drop correction of the CV scans, and results are presented by the dashed lines in Fig. 4a. The general feature of the potential sweep curves still remains the same, and for that reason, the non-corrected potential, U'_{WR}, has been used for further diagrams and discussion.

Figure 4b shows the recorded CO_2 and NO concentration changes during five consecutive voltammetric cycles, where the potential is cycled between −1.5 and +1.5 V with a scan rate of 30 mV s^{-1}. The time between two successive large CO_2 or NO peaks is 200 s. In each cycle the rates of CO_2 formation and NO reduction exhibits two maxima, the larger one corresponding to the electrophobic behaviour ($\partial r/\partial U > 0$) at positive potentials, and the smaller one corresponding to the smaller, in general, electrophilic behaviour ($\partial r/\partial U < 0$) at negative potentials. The rate enhancement in CO_2 and N_2 formation during every cycle is quite reproducible.

In Fig. 5, the imposed potential is presented as a function of time together with the time variation of CO_2 formation at 380 (open symbols) and 490 °C (filled symbols) for the last of the five consecutive cycles. The enhancement in the rates during anodic and cathodic potential sweep is more pronounced at lower scan rates and at higher temperatures. There is clearly a time delay between the maximum of the imposed potential and the obtained maximum concentration in CO_2, which is less pronounced at higher temperatures (filled circles) and at the smallest scan rate investigated. This indicates, as one would expect, a smaller departure from steady state at higher temperatures. The time variation of the CO_2 signal has been corrected by the residence time in the lines between the reactor and the CO_2 analyzer.

Figure 6 presents the cyclic variation of current and CO_2 and N_2 formation rates and the obtained rate enhancement ratios, ρ, values as a function of the imposed potential for different scan rates at 380 and 490 °C. By comparing these ρ values with those obtained under state polarization (Table 1) under the same conditions, it is observed that they are smaller (e.g. ρ_{CO_2} is 20 vs. 66 and ρ_{N_2} is 15 vs. 24 at 380 °C). This also implies that the time-averaged rate enhancement under forced oscillation conditions is smaller than under steady-state anodic or cathodic polarization at the vertex potential. This is due to the inverted volcano nature of the system manifested, e.g., in Fig. 4 right.

Figure 7 demonstrates the way in which Faradaic efficiencies, Λ, can be calculated during forced oscillation experiments. The diagram shows the cross plotted rate, r_{CO_2}, and absolute values of current as a function of the

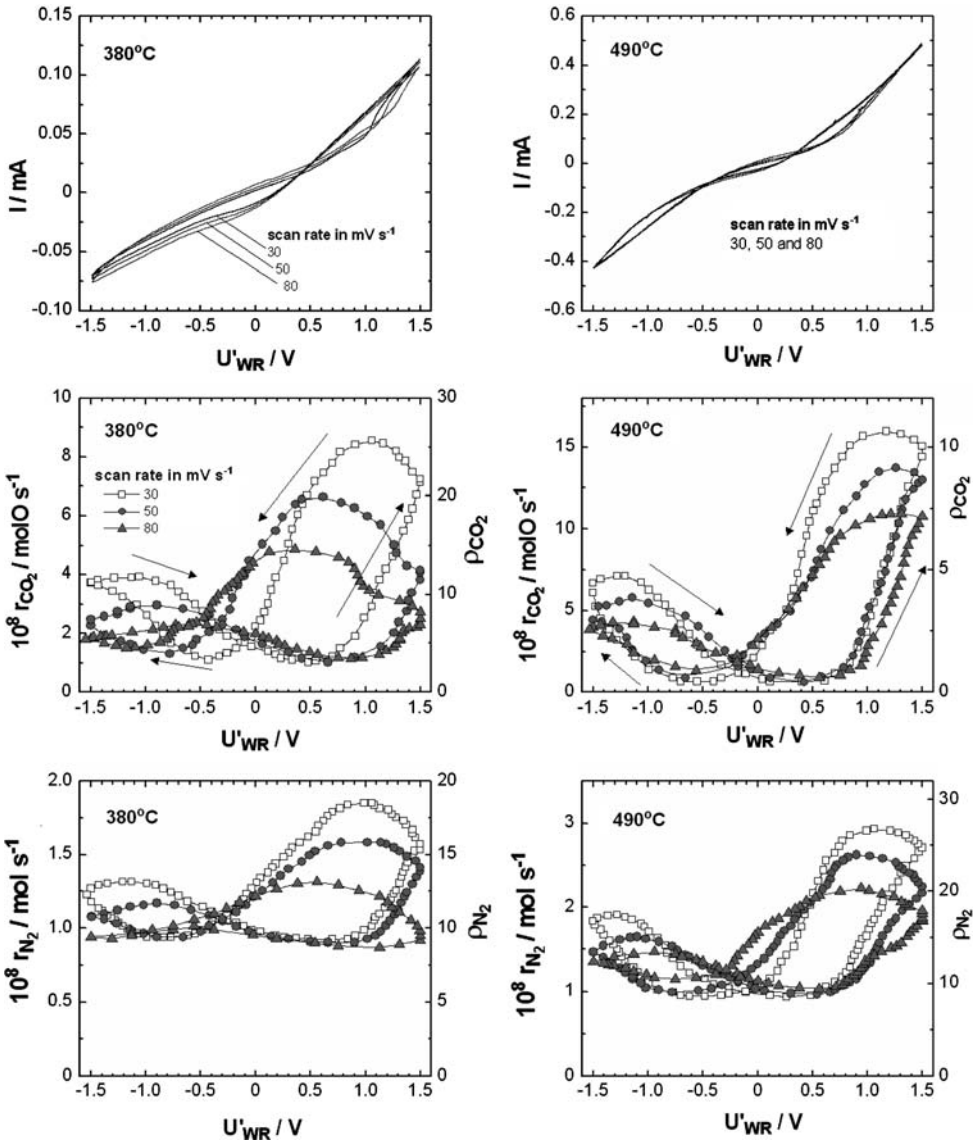

Fig. 6 Top: Cyclic voltammograms at 380 and 490 °C as a function of scan rate middle and bottom: Cyclic variation in the CO_2 and N_2 formation rates and rate enhancement ratios, ρ_{CO_2}, ρ_{N_2},with catalyst potential for 380 and 490 °C. Scan rate: (□) 30 mV s^{-1}, (●) 50 mV s^{-1}, and (▲) 80 mV s^{-1}. The last of five consecutive cycles is always shown. Conditions as in Fig. 1

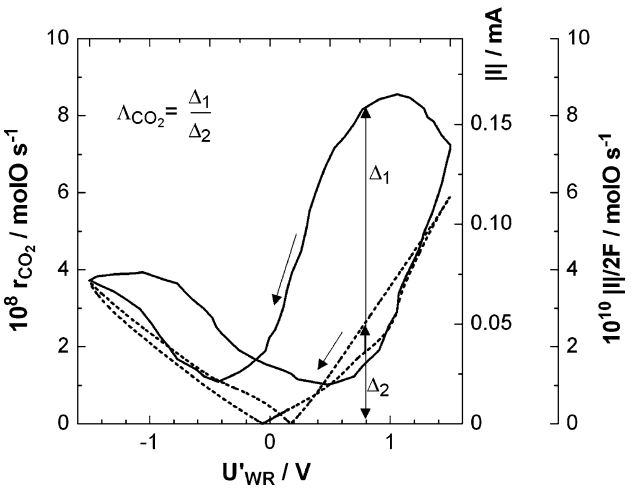

Fig. 7 Cyclic variation in the CO_2 formation rate and absolute values of current as a function of imposed catalyst potential at 380 °C. See text for discussion. Conditions as in Fig. 1

imposed potential. A third axis presenting I/2F is introduced, so that the ratio Δ_1 ($\Delta r_{CO_2} = 8 \times 10^{-8}$ mol O s^{-1}) to Δ_2 (I/2F = 2.5×10^{-10} mol O s^{-1}) gives a value of $\Lambda_{CO_2} \approx 320$. The estimation of Λ_{CO_2} for 380 °C based on the current exchange density, I_0, obtained from the Tafel plots of Fig. 3b, symbol (◇), and the open circuit rate, $r^o_{CO_2}$, via equation (1), i.e.:

$$\Lambda_{CO_2} = 2Fr^o_{CO_2}/I_0 \quad (6)$$

predicts a value of $\Lambda_{CO_2} \approx 200$, which is in good agreement with the experimental results of steady state and cyclic voltammetry studies.

4 Conclusions

Cyclic voltammetric investigation of electropromoted reactions is of significant practical and theoretical

interest. In the present study the appearance of the redox couple $Rh^0 \leftrightarrow Rh^{3+}$ hinders the detection of chemisorbed species. At medium scan rates SECV can serve as a useful initial test for electrochemically promoted NO reduction. Due to the inverted volcano nature of the NO reduction on Rh, the time-averaged rate enhancement is smaller than that corresponding to steady state anodic or cathodic polarization. It is very likely that for volcano-type reactions the time-averaged rate enhancement during SECV can exceed that one obtained under steady polarization conditions. This point is worth investigating in future studies.

References

1. Lintz H-G, Vayenas CG (1989) Angewandte Chemie Intern Ed in Engl 28(6):708
2. Vayenas CG, Bebelis S, Neophytides S, Yentekakis IV (1989) Appl Phys A 49:95
3. Nicole J, Tsiplakides D, Pliangos C, Verykios XE, Comninellis Ch, Vayenas CG (2001) J Catal 204:23
4. Pliangos C, Raptis C, Badas T, Tsiplakides D, Vayenas CG (2000) Electrochim Acta 46:331
5. Constantinou I, Archonta D, Brosda S, Lepage M, Sakamoto Y, Vayenas CG (2007) J Catal 251:400
6. Foti G, Lavanchy O, Comninellis Ch (2000) J Appl Electrochem 30:1223
7. Baranova EA, Fóti G, Comninellis Ch (2004) Electrochem Commun 6:389
8. Baranova EA, Thursfield A, Brosda S, Fóti G, Comninellis Ch, Vayenas CG (2005) J Electrochem Soc 152(2):E40
9. Tsiplakides D, Balomenou SP, A Katsaounis D Archonta C Kotsoudontis CG Vayenas (2005) Catal Tod 100:133
10. Balomenou SP, Tsiplakides D, Katsaounis A, Brosda S, Hammad A, Fóti G, Comninellis Ch, Thiemann-Handler S, Cramer B, Vayenas CG (2006), Solid State Ionics 177:2201
11. Vayenas CG, Brosda S, Pliangos C (2001) J Catal 203:329
12. Vayenas CG, Bebelis S, Pliangos C, Brosda S, Tsiplakides D (2001) Electrochemical activation of catalysis: promotion, electrochemical promotion and metal-support interactions. Kluwer Academic/Plenum Publishers, New York
13. Vayenas CG, Tsiplakides D (2000) Surf Sci 467:23
14. Chao T, Walsh KJ, Fedkiw PS (1991) Solid State Ionics 47:277
15. Jaccoud A, Fóti G, Comninellis Ch (2006) Electrochim Acta 51:1264
16. Jaccoud A, Falgairette C, Fóti G, Comninellis Ch (2007) Electrochim Acta 52:7927
17. Vayenas CG, Ioannides A, Bebelis S (1991) J Catal 129:67
18. Billard A, Vernoux P (2007) Top Catal 44(3):369
19. Bard AJ, Faulkner LR (2001) Electrochemical methods. John Wiley & Sons, Inc., New York